A Spherical Harmonics Shape Model for Level Set Segmentation

Maximilian Baust and Nassir Navab

Computer Aided Medical Procedures (CAMP),
Technische Universität München,
Boltzmannstr. 3, 85748 Garching, Germany
{baust,navab}@in.tum.de
http://campar.in.tum.de

Abstract. We introduce a segmentation framework which combines and shares advantages of both an implicit surface representation and a parametric shape model based on spherical harmonics. Besides the elegant surface representation it also inherits the power and flexibility of variational level set methods with respect to the modeling of data terms. At the same time it provides all advantages of parametric shape models such as a sparse and multiscale shape representation. Additionally, we introduce a regularizer that helps to ensure a unique decomposition into spherical harmonics and thus the comparability of parameter values of multiple segmentations. We demonstrate the benefits of our method on medical and photometric data and present two possible extensions.

Keywords: Segmentation, Level Set Methods, Variational Methods, Shape Models, Spherical Harmonics.

1 Introduction

Level set methods and particularly variational level set methods belong to the most flexible tools for image segmentation as far as the modeling of data terms and the handling of topological changes during the evolution are concerned. However, this topological flexibility may be undesired for two reasons:

- The object boundaries are not clearly defined by strong image gradients or significant changes in the intensity distribution, which occurs especially for many medical applications, where image data often suffers from low tissue contrast or noise. Thus the contour may *leak* into surrounding objects.
- The evolution might get stuck in an undesired local minimum. Thus the segmentation problem needs additional regularization in order to pick out the desired minimum.

In contrast to topologically flexible level set methods, parametrized active contours allow to add the required amount of regularity to such problems as illustrated in Fig. 1. We distinguish three classes of parametrized active contours,

K. Daniilidis, P. Maragos, N. Paragios (Eds.): ECCV 2010, Part III, LNCS 6313, pp. 580–593, 2010.

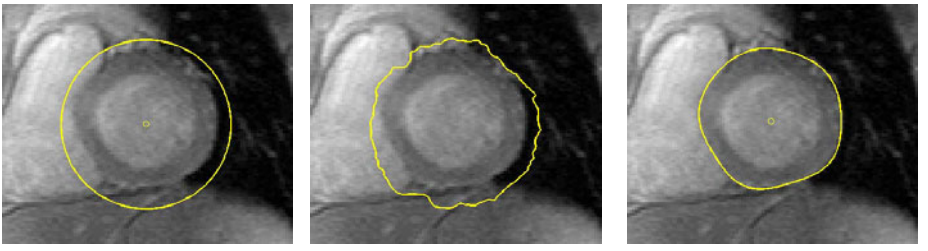

(a) initialization (b) Sobolev flow (c) proposed method

Fig. 1. The Benefit of a Parametric Shape Model: The segmentation of the outer wall of the left ventricle acquired with magnetic resonance imaging [1] with a Sobolev gradient flow (cf. Sec. 5) gets stuck in an undesired local minimum (b). In contrast to this, the proposed approach clearly benefits from the employed shape model (c).

no matter whether they use an explicit or implicit surface representation: Methods using a *parametrized surface description*, methods based on *statistical shape models* and methods employing a *parametric shape model*. The first class consists of methods that only have a parametrized surface description, but no model based assumption about the topology of the shape to be segmented. Popular examples are all kinds of topology-adaptive and generalized snakes, which can be subsumed under *deformable models* [2]. The second and the third class are represented by all approaches employing a statistical or a parametric shape model. In both cases the object is represented as a linear combination of basis functions. While for statistical shape models these basis functions are generated from training data and are thus application specific, parametric shape models employ a fixed set of basis functions such as spherical harmonics or wavelets for instance. Of course, many methods based on parametric shape models also use training data in order to adapt the shape model to the specific application by constraining the parameters as it is done in [3], [4], [5], [6], and [7].

However, there are situations where one would like to use a parametric shape model even when no training data is available. The method we propose combines an implicit surface representation with a parametric shape model based on spherical harmonics. Moreover, we propose a regularizer which helps to ensure a unique decomposition into spherical harmonics and thus the comparability of several segmentations, if no training data is available. In detail, our method inherits the following advantages from implicit representations:

- In contrast to explicit surface representations no remeshing of the surface during the evolution is necessary.
- Cost function evaluations, especially for region-based data terms, can be computed very easily using smeared-out versions of the Heaviside function and its derivatives, because the membership of every pixel to fore- or background is automatically given by the level set function.
- The proposed framework inherits the full flexibility of variational level set methods regarding the modeling of region- and surface-based data terms.

Table 1. Overview over Parametrized Active Contours: Our method combines an implicit surface representation with a parametric shape model as well as the advantages from both of them

shape model	**none**	**statistical**	**parametric**
explicit shape representation	Deformable Models (e.g. Terzopoulos in [2])	Active Shape Models (e.g. Cootes et al. [8])	Staib and Duncan [3], Székely et al. [4], Kelemen et al. [5], Nain et al. [6], Yu et al. [7]
implicit shape representation	Huang et al. [9] (MetaMorphs), Morse et al. [10], Ho et al. [11], Slabaugh et al. [12]	Leventon et al. [13], Tsai et al. [14]	**our method**

Moreover, the presented method also inherits advantages from the employed parametric shape model and the proposed regularizer:

- In contrast to traditional level set methods, the parametrization removes the necessity for the level set function to be a signed distance function in order to avoid numerical problems.
- The spherical harmonics parametrization provides a sparse and multiscale surface description.
- The proposed regularizer helps to ensure a unique decomposition of spherical harmonics, if no training data is available. This makes it possible to compare the parameters of several segmentations, which is helpful for creating an atlas for instance.

Concisely put, the proposed method combines advantages from both implicit surface representations and parametric shape models.

1.1 Related Work

As illustrated in Tab. 1, our method is a missing link in the field of parametrized active contours, because it combines a parametric shape model (based on spherical harmonics) with an implicit surface representation. Related methods have either no parametric shape model, or no level set representation. Note that traditional level set methods are not discussed in this context as they do not feature a parametrization.

Methods Employing no Parametric Shape Model. All methods with a parametrized surface description based on splines or NURBS and an explicit contour representation are referred to as *deformable models* [2]. Besides these methods employing an explicit surface representation, there are several publications on parametrized implicit contours. In 2004 Huang et al. have published their MetaMorphs framework, where a grid of control points is attached to the level set function, which is then deformed via free-from deformations [9]. Level

set functions parametrized by radial basis functions have been investigated by Morse et al. [10] and Slabaugh et al. [12] in 2005 and 2007, respectively. Also, in 2005 Ho et al. [11] have suggested to use an unstructured point cloud for discretizing the level set function.

Methods Employing a Statistical Shape Model. As explained above, methods employing a statistical shape model represent the shape using basis functions computed from training data. This makes them very flexible as far as the shape of the object is concerned, but it requires training data for every new application. In 1992 Cootes and Taylor have introduced the so-called *active shape models* or *smart snakes*, characterized by an explicit surface representation (see Cootes et al. [8] for a detailed description). Similar approaches using an implicit contour representation have been developed by Leventon et al. [13] and Tsai et al. [14] in 2000 and 2003, respectively.

Methods Employing a Parametric Shape Model. In 1996 Staib and Duncan have used Fourier surfaces to describe objects with open and closed surface as well as tori and tubes [3]. Also in 1996 Székely et al. have published their framework for segmenting objects with spherical topology [4]. Therefore they discretize the object by a mesh, which is then mapped onto the unit sphere and parametrized by spherical harmonics. Kelemen et al. have used a similar approach in [5] (1999). Recently, these methods have found their counterparts based on spherical wavelets, which have been published by Nain [6] and Yu [7] in 2007. It is important to notice, that all of these methods employ an explicit surface representation and require training data.

1.2 Outline

The remainder of this work is organized as follows. Section 2 describes how the implicit contour representation is combined with the parametric shape model. After that we explain how to use the derived level set framework with exemplary surface- and region-based data terms in section 3. Additionally, we derive a regularizer that helps to ensure a unique decomposition into spherical harmonics while providing the ability to incorporate prior information, if necessary. All necessary information for implementing our method is given in section 4. In section 5 we discuss all performed experiments. Finally, section 6 is dedicated to the conclusion.

2 Level Set Framework

Before explaining how a parametric shape model based on spherical harmonics can be combined with a level set representation, we recap the concept of spherical coordinates. The boundary of any (two- or three-dimensional) *stellar* or *star-shaped* object (see Fig. 2 for explanation) can be described by

$$r(\theta, \varphi) \cdot s(\theta, \varphi), \tag{1}$$

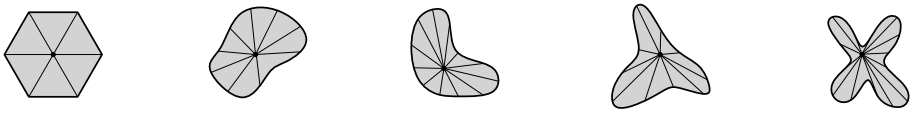

(a) (b) (c) (d) (e)

Fig. 2. Examples for Star-shaped Objects: *Star-shaped* or *stellar* objects consist of one connected component, with at least one point in the interior from which the whole boundary of the object can bee seen

where $r : [0, \pi] \times [0, 2\pi) \to [0, +\infty)$ is the radius (function) scaling the corresponding unit vector

$$s(\theta, \varphi) = (\sin(\theta)\cos(\varphi), \sin(\theta)\sin(\varphi), \cos(\theta))^T, \tag{2}$$

as shown in Fig. 3(a). $\theta \in [0, \pi]$ is called *inclination angle* and $\varphi \in [0, 2\pi)$ is called *azimuth angle*. In the two-dimensional case θ equals $\pi/2$ and we simply write $r(\varphi) = r(\pi/2, \varphi)$.

2.1 Contour Representation

In the following we denote the image domain by $\Omega \subset \mathbb{R}^d$ $(d = 2, 3)$ and the embedding function by $\phi : \Omega \to \mathbb{R}$. First, we consider the case of segmenting a ball $B_r(c)$ with constant radius r and center point $c \in \mathbb{R}^d$. In this case, ϕ can be written as

$$\phi(x) = |x - c| - r \tag{3}$$

such that the zero level set of ϕ describes the surface of $B_r(c)$. By allowing r to be dependent on $\theta = \theta(x)$ and $\varphi = \varphi(x)$ we can now segment any star-shaped object:

$$\phi(x) = \begin{cases} |x - c| - r(\theta(x), \varphi(x)), & x \neq c, \\ \inf_{x \neq c} \phi(x), & x = c. \end{cases} \tag{4}$$

In order to keep the notation simple, we will omit the argument x from θ and φ in the following. Before we continue with the parametric shape model, the following two points are important to notice:

- The radius r depends on the position of the center point c as illustrated in Fig. 3(b) and 3(c). Thus, if a unique representation is needed, e.g. in order to compare two segmentations, we need a regularizer that helps to ensure this unique representation. We will discuss this issue in detail in subsection 3.2.
- ϕ has a singularity at $x = 0$. This singularity, however, only affects the vicinity of a few pixels and is thus not an issue for real applications as depicted in Fig. 4. Moreover, traditional level set methods require the embedding function to be a signed distance function in order to avoid shocks causing

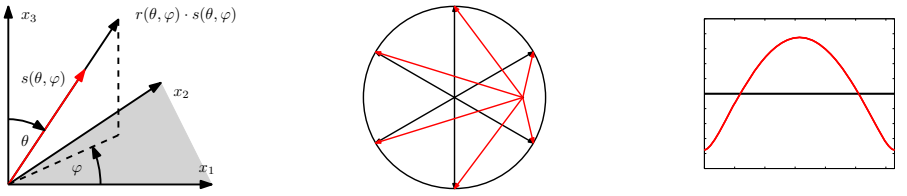

(a) (b) (c) r

Fig. 3. Spherical Coordinates and their Dependency on the Center Point: The radius $r(\theta, \phi)$ (a) depends on the position of the center point (b) as visualized in (c). Thus a regularizer is required, if a unique representation is needed (see Sec. 3.2).

numerical problems during the evolution [15]. Of course, ϕ in the form of (4) is not necessarily a signed distance function (see also Fig. 4), but since ϕ is parametrized via $r(\theta, \varphi)$, there is no need for maintaining this property.

2.2 Parametric Shape Model

The level set representation (4) can now be combined with any parametrization of $r(\theta, \varphi)$, such as double Fourier series, spherical harmonics, or spherical wavelets. However, in contrast to double Fourier series for instance, spherical harmonics have the advantage that no care has to be taken for ensuring correct boundary conditions at the poles. Thus we approximate r with a truncated spherical harmonics expansion [16]:

$$r(\theta,\varphi) \approx \sum_{l=0}^{N} \{r_l^0 \cdot P_l^0(\cos(\theta)) + \sum_{m=1}^{l} [a_l^m \cdot \cos(m\varphi) + b_l^m \cdot \sin(m\varphi)] \cdot P_l^m(\cos(\theta))\}, \quad (5)$$

where P_l^m denotes the associated Legendre Polynomial of degree l and order m. In the two-dimensional case (5) boils down to a Fourier expansion of the form

$$r(\theta,\varphi) \approx r_0^0 + \sum_{l=1}^{N} [a_l^l \cdot \cos(l\varphi) + b_l^l \cdot \sin(l\varphi)], \quad (6)$$

because for $\theta = \pi/2$ we have

$$P_l^m(\cos(\theta)) = P_l^m(0) = \begin{cases} 0, & m < l \\ 1, & m = l \end{cases}. \quad (7)$$

3 Variational Formulation

In this section we show how the level set framework introduced in the last section can be combined with variational level set formulations. Further, we explain how to regularize the level set evolution in order to obtain a unique decomposition into spherical harmonics.

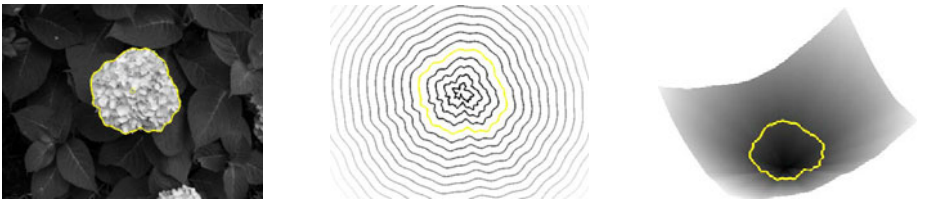

(a) segmentation (b) contours of ϕ (c) surface plot of ϕ

Fig. 4. A First Example: Segmentation of a flower (a), taken from [17], and a contour plot (b) as well as a surface plot (c) of the embedding function

3.1 Data Terms

The derived level set framework can be combined with arbitrary data terms for variational level set methods. Since the discussion of all possible variational data terms is far beyond the scope of this work, we only consider widely used representatives of surface- and region-based energies.

For the remainder of this work $I : \mathbb{R}^d \to \mathbb{R}$ denotes the image or volume containing the object to be segmented. A well-known surface-based energy is the *geodesic active contour model*

$$\mathcal{G}(\phi) = \int_\Omega \delta(\phi)|\nabla\phi| g \, dx, \tag{8}$$

where g is an *edge-indicator function* such as

$$g(x) = (1 + |\nabla I(x)|^2)^{-1}, \tag{9}$$

which was used by Caselles et al. in [18]. Often, surface-based energies are combined with a region-based ones like the *weighted area term* [15]

$$\mathcal{A}(\phi) = \int_\Omega H(-\phi) g \, dx \tag{10}$$

for forcing the contour either to shrink, or to expand. Another well-known region-based energy is the one proposed by Chan and Vese in [19]

$$\mathcal{P}(\phi) = \int_\Omega H(-\phi)(I - \mu_i)^2 + H(\phi)(I - \mu_o)^2 \, dx, \tag{11}$$

where μ_i and μ_o denote the mean intensity values inside and outside the contour. We denote the linear combination of these three data terms by

$$\mathcal{D}(\phi) = \lambda_G \mathcal{G}(\phi) + \lambda_A \mathcal{A}(\phi) + \lambda_P \mathcal{P}(\phi), \tag{12}$$

where λ_G, λ_A, and λ_P control the influence of each term. While $\lambda_A > 0$ results in a shrinking contour, $\lambda_A < 0$ forces the contour to expand. All these parameters are easy to adjust as shown in Tab. 2.

3.2 Regularization

For many examples a minimization of $\mathcal{D}(\phi)$ using the parametrized embedding function ϕ would already provide us with meaningful segmentation results. However, if we want to use the found coefficients r_l^0, a_l^m, and b_l^m for generating an atlas or if we want to compare them with coefficients of another segmentation, we have to ensure their uniqueness as also illustrated in Fig. 3. Uniqueness of the parameters can be achieved by constraining the radius function. The reason is that any constraint on the radius function is also a constraint on the center and thus a unique decomposition is guaranteed.

At a first glance

$$\frac{1}{2}\left\|\nabla_{(\theta,\varphi)} r\right\|_{L_2}^2 \stackrel{!}{=} \min \tag{13}$$

might seem to be a reasonable constraint, because smoothness constraints are often used as regularizers. In our case (13) is not a good choice, because r_0^0 is not constrained as $\nabla_{(\theta,\varphi)} r$ does not depend on r_0^0. Instead, by penalizing the L^2-norm of the radius function

$$\frac{1}{2}\|r\|_{L^2}^2 = \frac{1}{2}\int_0^{2\pi}\int_0^{\pi} |r(\theta,\varphi)|^2 \, d\theta \, d\varphi \stackrel{!}{=} \min \tag{14}$$

we achieve a unique decomposition into spherical harmonics, because applying Parselval's theorem [16] to (14) yields

$$\frac{1}{2}\|r\|_{L^2}^2 = \frac{1}{2}\sum_{l=0}^{N}\{(r_l^0)^2 + \sum_{m=1}^{l}[(a_l^m)^2 + (b_l^m)^2]\} \stackrel{!}{=} \min . \tag{15}$$

Obviously all coefficients are constrained now. Moreover, (14) allows the following two interpretations.

Let $\bar{x} \in \Omega$ denote the center of mass of the object defined by r. Then

$$\bar{x} = \frac{1}{2\pi^2}\int_0^{2\pi}\int_0^{\pi} c + r(\theta,\varphi)\cdot s(\theta,\varphi) \, d\theta \, d\varphi \tag{16}$$

$$= c + \frac{1}{2\pi^2}\int_0^{2\pi}\int_0^{\pi} r(\theta,\varphi)\cdot s(\theta,\varphi) \, d\theta \, d\varphi \tag{17}$$

From (17) we deduce that

$$\|\bar{x} - c\|_2^2 \leq \frac{1}{2\pi^2}\|r\|_{L^2}^2 , \tag{18}$$

which means that (14) has the nice side-effect, that it attracts c towards the center of mass. This can also help to prevent the level set evolution from getting stuck in local minima.

Rewriting (14) as

$$\frac{1}{2}||r||_{L^2}^2 = \frac{1}{2}||r-0||_2^2 \tag{19}$$

yields the second interpretation. Obviously (14) forces r to be close to 0 and that is why severe over-regularization might result in a shrinking contour. However,

(a) initialization (b) Sobolev flow (c) proposed method

(d) initialization (e) Sobolev flow (f) proposed method

Fig. 5. Adding Regularity: If the object of interested is star-shaped, the additional regularity provided by the shape model helps to avoid undesired local minima. Note that the Sobolev flow minimizes the same energy. Both examples are taken from [17].

by replacing 0 with a known radius function $\hat{r}$ prior shape information can be incorporated. Of course, in this case θ and φ have to be replaced by $\theta + \theta_0$ and $\varphi + \varphi_0$, where θ_0 and φ_0 are additional phase angles, that allow us to optimize for rotations as well. An example for this situation is shown in Fig. 6.

3.3 The Complete Model

Combining the data term (12) and the regularizer (14), we obtain the following minimization problem characterizing the optimal configuration of the surface:

$$\min_{\phi,r} \mathcal{E}(\phi, r), \quad \text{where} \quad \mathcal{E}(\phi, r) = \mathcal{D}(\phi) + \frac{\lambda_R}{2} \|r\|^2_{L_2}. \tag{20}$$

4 Numerical Solution

We minimize (20) using a gradient descent approach, whose details will be described in Sec. 4.1. In Sec. 4.2 we give some details on the implementation and in Sec. 4.3 we discuss the parameter settings and the initialization of the contour.

4.1 Gradient Descent

Let p denote one of the parameters r_l^0, a_l^m, b_l^m, or c_j ($c = (c_1, c_2, c_3)^T$) and ∂_p the partial derivative with respect to p. For every parameter p we perform a fixed number of steepest descent steps $i = 0, 1, 2, \ldots$:

$$p^{i+1} = p^i - \tau \cdot \partial_p \mathcal{E}(\phi, r). \tag{21}$$

(a) initialization (b) 10 steps (c) 50 steps (d) 100 steps (e) 250 steps

Fig. 6. Incorporating Prior Knowledge: By incorporating prior information into the regularizer we can initialize the level set function arbitrarily and segment the destroyed object successfully

It is important to notice that we perform the steepest descent *simultaneously for all parameters* and that we use the *same* step size τ for all of them. The main reason for this fact is, that r_l^0, a_l^m and b_l^m contribute to the shape of the surface in equal shares. This is not the case when using complex-valued spherical harmonics, where the parameters are the amplitudes and phase shifts, which have not the same units. Further, also the mean values μ_i and μ_o in (11) are updated in every step (cf. [19]).

In order to optimize the phase parameters $p = \theta_0$ and $p = \varphi_0$ (cf. Fig. 6) we recommend to use a modified version of (21):

$$p^{i+1} = p^i - \tau \cdot \operatorname{sign}(\partial_p \mathcal{E}(\phi, r)) \min(|\partial_p \mathcal{E}(\phi, r)|, C), \tag{22}$$

where C is a positive constant restricting the maximal angle change per step to $\tau \cdot C$. In the example of Fig. 6 we set $C = 0.5$ and $\tau = 0.02$.

4.2 Details on the Implementation

In all our experiments we normalized the image intensities to the range $[0, 1]$. Further, we replaced ∇I in (9) by $\nabla(G * I)/\sigma$, where G is a truncated Gaussian kernel with window size 3 and standard deviation 0.5. The only differential operator necessary for computing $\partial_p \mathcal{E}(\phi, r)$ is ∇, which can be approximated using central differences. For computing $\partial_p \mathcal{E}(\phi, r)$ we also require approximations of $H(\phi)$, $\delta(\phi)$, and $\delta'(\phi)$ and we employed their smeared-out versions as suggested by Osher and Fedkiw in [20].

4.3 Initialization and Parameter Choice

The easiest way of initializing the level set evolution consists of defining an initial ball. It is also possible to let the user specify an initial polyhedron which can be easily approximated by spherical harmonics as done in Fig. 6. As far as the choice of the parameters N, λ_G, λ_A, λ_P, λ_R, τ, and σ is concerned we can deduce from Tab. 2 that they do not vary significantly from one experiment to another. The step size τ has to be chosen approximately an order of magnitude smaller when performing segmentations in three dimensions, because the data term $\mathcal{D}(\phi)$ scales with the size of the zero level set.

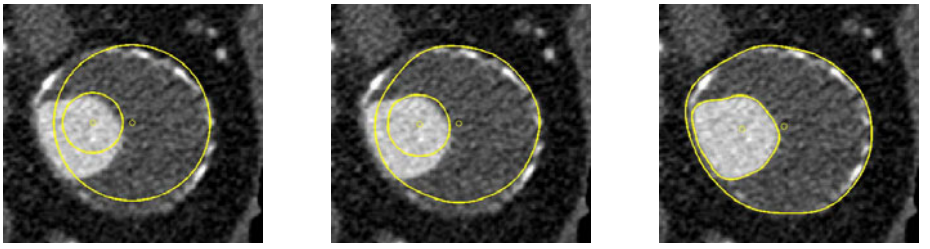

(a) initialization (b) 10 steps (c) 100 steps

Fig. 7. Simultaneous Segmentation: We segment the inner and outer wall of an abdominal aortic aneurysm using two level set functions evolved simultaneously by the coupled Chan-Vese model described in Sec. 5.3

5 Experiments

We performed several experiments to demonstrate the potential of our method. The used parameter values can be found in Tab. 2.

5.1 Two Dimensional Experiments

We compared our results with a topological flexible level set method and we used a *Sobolev gradient flow* [21]

$$\phi(x, t+\tau) = \phi(x,t) - \tau \cdot (I - \Delta)^{-1} \nabla \mathcal{D}(\phi), \tag{23}$$

where $\nabla \mathcal{D}(\phi)$ is defined as

$$\frac{d}{dh} \mathcal{D}(\phi + h \cdot \psi)\Big|_{h=0} = \int_\Omega \nabla \mathcal{D}(\phi) \psi \, dx. \tag{24}$$

The experiments in Fig. 1 as well as Fig. 5 clearly show that, if the object to be segmented is star-shaped, the parametric shape model and the proposed regularizer add meaningful information to the problem. It is important to notice that *both* methods - the Sobolev flow and our method - minimize the *same* data term.

5.2 Three Dimensional Experiments

The applicability of our method to three dimensional medical applications is presented in Fig. 8. We segmented five abdominal aortic aneurysms (AAAs) from computed tomography angiography (CTA) data. An AAA is a pathological dilation of the lumen in the abdominal part of the aorta, which may rupture, if left untreated. Among others, the maximum diameter is used as an indicator for estimating the rupture risk. Since a segmentation of these AAAs is not only beneficial for diagnosis, but also for treatment planning, this application is of great

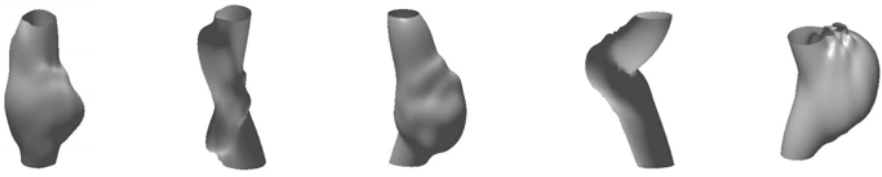

(a) (b) (c) (d) (e)

Fig. 8. 3D Experiments: The segmentation of abdominal aortic aneurysms with our method shows that our method is able to capture the large anatomical variability

relevance. Thanks to the proposed regularizer, the parameter values r_l^0, a_l^m and b_l^m contain meaningful shape information, which could be used for automated diagnosis. As visible in Fig. 8 our method performs well in capturing the large variability of these AAAs.

5.3 Possible Extensions

Fig. 6 shows the incorporation of prior information into the level set evolution by replacing (14) with

$$\frac{1}{2}\left\|r-\hat{r}\right\|_{L_2}^2 \stackrel{!}{=} \min, \tag{25}$$

where $\hat{r}$ is obtained from a segmentation of an unspoilt image. This example shows that our method is not only modular and flexible as far as the choice of data terms is concerned, but also with respect to the employed regularizer. As a suggestion for future research, one could also think of including statistical information about $\hat{r}$.

Another possible extension is shown in Fig. 7, where we minimized the following coupled Chan-Vese model in order to segment the inner and the outer wall of an abdominal aorta acquired by computed tomography angiography:

$$\mathcal{D}(\phi_i) = \int_\Omega H(-\phi_i)[(I-\mu_i)^2 + \lambda H(\phi_o)] + H(\phi_i)H(-\phi_o)(I-\mu_m)^2\,dx, \tag{26}$$

$$\mathcal{D}(\phi_o) = \int_\Omega H(-\phi_o)H(\phi_i)(I-\mu_m)^2 + H(\phi_o)[(I-\mu_o)^2 + \lambda H(-\phi_i)]\,dx, \tag{27}$$

where ϕ_i is the level set function corresponding to the inner contour and ϕ_o is the level set function corresponding to the outer contour. Consequently μ_i is the mean intensity value inside both contours, μ_m is the mean intensity between both contours, and μ_o is the mean intensity value outside both contours. Thus we are able to segment the lumen as well as the thrombus of an AAA *simultaneously*.

Table 2. Parameters used

Fig.	N	λ_G	λ_P	λ_A	λ_R	σ	τ	τ (Sobolev)	steps
1(a)	5	1	0	0.1	0.1	0.04	0.02	20	100
4(a)	25	0.1	1	0	0.02	0.045	0.02	-	100
5(a)	20	0.3	1	0	0.1	0.1	0.01	20	500
5(d)	15	0.2	1	0	0.1	0.6	0.02	30	500
6	25	0.2	1	0	6	0.023	0.02	-	250
7	8	0	1	0	0.02	-	0.01	-	100
8	12	0.25	1	-0.3	0.1	0.023	0.001	-	500

6 Conclusion

We have introduced a missing link in the field of parametric active contours which combines advantages of both implicit active contours and parametric shape models. The great flexibility with respect to the choice of data terms and the ability to work also in three dimensions make the proposed method valuable for many, especially medical, applications. Another benefit of our method is the proposed regularizer, which constraints the parameters in a meaningful way and allows to incorporate prior information very easily. We hope that, due to the presented extensions and the ability to combine the proposed method also with other shape models, such as spherical wavelets for instance, our work could serve as a fruitful basis for further research and applications.

Acknowledgments. The first author is funded by the International Graduate School of Science and Engineering at Technische Universität München. Moreover, the authors would like to thank Darko Zikic for many valuable comments.

References

1. Stegmann, M.B.: An annotated dataset of 14 cardiac MR images. Technical report, Informatics and Mathematical Modelling, Technical University of Denmark, DTU (2002)
2. Osher, S., Paragios, N.: Geometric Level Set Methods in Imaging,Vision,and Graphics. Springer, Heidelberg (2003)
3. Staib, L., Duncan, J.: Model-based deformable surface finding for medical images. Medical Imaging, IEEE Transactions on 15, 720–731 (1996)
4. Székely, G., Kelemen, A., Brechbühler, C., Gerig, G.: Segmentation of 2-d and 3-d objects from mri volume data using constrained elastic deformations of flexible fourier contour and surface models. Medical Image Analysis 1, 19–34 (1996)
5. Kelemen, A., Szekely, G., Gerig, G.: Elastic model-based segmentation of 3-d neuroradiological data sets. Medical Imaging, IEEE Transactions on 18, 828–839 (1999)
6. Nain, D., Haker, S., Bobick, A., Tannenbaum, A.: Multiscale 3-d shape representation and segmentation using spherical wavelets. IEEE Transactions on Medical Imaging 26, 598–618 (2007)

7. Yu, P., Grant, P., Qi, Y., Han, X., Segonne, F., Pienaar, R., Busa, E., Pacheco, J., Makris, N., Buckner, R., Golland, P., Fischl, B.: Cortical surface shape analysis based on spherical wavelets. IEEE Transactions on Medical Imaging 26, 582–597 (2007)
8. Cootes, T., Taylor, C., Cooper, D., Graham, J.: Active shape models - their training and application. Computer Vision and Image Understanding 61, 38–59 (1995)
9. Huang, X., Metaxas, D., Chen, T.: Metamorphs: Deformable shape and texture models. In: Proceedings of the 2004 IEEE Computer Society Conference on Computer Vision and Pattern Recognition, CVPR 2004, vol. 1, pp. I–496 – I–503 (2004)
10. Morse, B., Liu, W., Yoo, T., Subramanian, K.: Active contours using a constraint-based implicit representation. In: IEEE Computer Society Conference on Computer Vision and Pattern Recognition, CVPR 2005., vol. 1, pp. 285–292 (2005)
11. Ho, H.P., Chen, Y., Liu, H., Shi, P.: Level set active contours on unstructured point cloud. In: IEEE Computer Society Conference on Computer Vision and Pattern Recognition, CVPR 2005., vol. 2, pp. 655–662 (2005)
12. Slabaugh, G., Dinh, Q., Unal, G.: A variational approach to the evolution of radial basis functions for image segmentation, pp. 1 –8 (2007)
13. Leventon, M., Grimson, W., Faugeras, O.: Statistical shape influence in geodesic active contours. In: Proceedings of IEEE Conference on Computer Vision and Pattern Recognition, vol. 1, pp. 316–323 (2000)
14. Tsai, A., Yezzi Jr., A., Wells, W., Tempany, C., Tucker, D., Fan, A., Grimson, W., Willsky, A.: A shape-based approach to the segmentation of medical imagery using level sets. IEEE Transactions on Medical Imaging 22, 137–154 (2003)
15. Li, C., Xu, C., Gui, C., Fox, M.: Level set evolution without re-initialization: a new variational formulation. In: IEEE Computer Society Conference on Computer Vision and Pattern Recognition, CVPR 2005, vol. 1, pp. 430–436 (2005)
16. Groemer, H.: Geometric Applications of Fourier Series and Spherical Harmonics. Cambridge University Press, Cambridge (1996)
17. Alpert, S., Galun, M., Basri, R., Brandt, A.: Image segmentation by probabilistic bottom-up aggregation and cue integration. In: IEEE Conference on Computer Vision and Pattern Recognition, CVPR 2007, pp. 1–8 (2007)
18. Caselles, V., Kimmel, R., Sapiro, G.: Geodesic active contours. Int. J. Comput. Vision 22, 61–79 (1997)
19. Chan, T., Vese, L.: Active contours without edges. IEEE Transactions on Image Processing 10, 266–277 (2001)
20. Osher, S., Fedkiw, R.: Level Set Methods and Dynamic Implicit Surfaces. Springer, Heidelberg (2003)
21. Sundaramoorthi, G., Yezzi, A.J., Mennucci, A.: Sobolev active contours. International Journal of Computer Vision 73, 345–366 (2007)